NIH Public Access
Author Manuscript
Toxicol Appl Pharmacol. Author manuscript; available in PMC 2015 January 01.

Published in final edited form as:
Toxicol Appl Pharmacol. 2014 January 1; 274(1): . doi:10.1016/j.taap.2013.10.029.

CYP2E1-Dependent and Leptin-Mediated Hepatic CD57 Expression on CD8+ve T Cells aid Progression of Environment-Linked Nonalcoholic Steatohepatitis

Ratanesh Kumar Seth[1], **Suvarthi Das**[1], **Ashutosh Kumar**[2], **Anindya Chanda**[1], **Maria B. Kadiiska**[2], **Gregory Michelotti**[3], **Jose Manautou**[4], **Anna Mae Diehl**[3], and **Saurabh Chatterjee**[1,*]

[1]Environmental Health and Disease Laboratory, Department of Environmental Health Sciences, Arnold School of Public Health, University of South Carolina, Columbia SC 29208

[2]Free Radical Metabolism Group, Laboratory of Toxicology and Pharmacology, National Institute of Environmental Health Sciences, Research Triangle Park, NC 27709

[3]Division of Gastroenterology, Duke University, Durham NC 27707

[4]Dept. of Pharmaceutical Sciences, University of Connecticut, Storrs, CT 06269-3092

Abstract

Environmental toxins induce a novel CYP2E1/leptin signaling axis in liver. This in turn activates a poorly characterized innate immune response that contributes to nonalcoholic steatohepatitis (NASH) progression. To identify the relevant subsets of T-lymphocytes in CYP2E1-dependent, environment-linked NASH, we utilized a model of diet induced obese (DIO) mice that are chronically exposed to bromodichloromethane. Mice deficient in CYP2E1, leptin (ob/ob mice), or both T and B cells (Pfp/Rag2 double knockout (KO) mice) were used to delineate the role of each of these factors in metabolic oxidative stress-induced T cell activation. Results revealed that elevated levels of lipid peroxidation, tyrosyl radical formation, mitochondrial tyrosine nitration and hepatic leptin as a consequence of metabolic oxidative stress caused increased levels of hepatic CD57, a marker of peripheral blood lymphocytes including NKT cells. CD8+CD57+ cytotoxic T cells but not CD4+CD57+ cells were significantly decreased in mice lacking CYP2E1 and leptin. There was a significant increase in the levels of T cell cytokines IL-2, IL-1β, IFN-γ in bromodichloromethane exposed DIO mice but not in mice that lacked CYP2E1, leptin or T and B cells. Apoptosis as evidenced by TUNEL assay and levels of cleaved caspase-3 was significantly lower in leptin and Pfp/Rag2 KO mice and highly correlated with protection from NASH. The

© 2013 Elsevier Inc. All rights reserved.

[1]**Author for correspondence:**Dr. Saurabh Chatterjee, Ph.D. Environmental Health and Disease Laboratory, Department of Environmental Health Sciences, University of South Carolina, Columbia 29208 USA. schatt@mailbox.sc.edu; Tel: 803-777-8120; Fax: 803-777-3391.

Publisher's Disclaimer: This is a PDF file of an unedited manuscript that has been accepted for publication. As a service to our customers we are providing this early version of the manuscript. The manuscript will undergo copyediting, typesetting, and review of the resulting proof before it is published in its final citable form. Please note that during the production process errors may be discovered which could affect the content, and all legal disclaimers that apply to the journal pertain.

Authorship: R.S. designed, performed experiments and statistical analysis of data. S.D. and, A.K. performed experiments. S.D analyzed data. A.C. performed experiments and analyzed microscopic images; M.B.K, G.M. and A.D. analyzed data and edited manuscript. S.C designed and performed experiment, analyzed data, wrote and edited manuscript.

"This article may be the work product of an employee or group of employees of the National Institute of Environmental Health Sciences (NIEHS), National Institutes of Health (NIH), however, the statements, opinions or conclusions contained therein do not necessarily represent the statements, opinions or conclusions of NIEHS, NIH or the United States government."

Conflict of interest: The authors declare no conflict of interest.

NIH-PA Author Manuscript
NIH-PA Author Manuscript
NIH-PA Author Manuscript

NIH-PA Author Manuscript

NIH-PA Author Manuscript

NIH-PA Author Manuscript

results described above suggest that higher levels of oxidative stress-induced leptin mediated CD8+CD57+ T cells play an important role in the development of NASH. It also provides a novel insight of immune dysregulation and may be a key biomarker in NASH.

Keywords

bromodichloromethane; lipid peroxidation; fibrosis; apoptosis; CD3; P53; caspase-3; TUNEL; IL-2; OB/OB mice

Introduction

Incidences of nonalcoholic steatohepatitis (NASH), a hepatic manifestation of metabolic syndrome and inflammation have increased in the last decade (1). This correlates with the rise in obesity to alarming proportions not only in the western world, but in developing countries like India, Brazil and China (2–4). Many laboratories in the past including our laboratory have hypothesized the involvement of environmental toxicants as a probable cause for NASH (5, 6). Recent published reports from our laboratory indicate the involvement of carbon tetrachloride and disinfection byproducts of drinking water bromodichloromethane (BDCM) and their free radical metabolism are possible factors for the progression of NASH (6–9). The metabolic oxidative stress generated from the exposure of these compounds, hasten the progression from steatosis to a more aggressive inflammatory pathophysiology associated with NASH development (6). Similarly it has been shown that CYP2E1 is the principle isoform among CYP450 enzymes in the liver that aid in NASH progression either through its generation of reactive oxygen species or by producing free radical metabolites of environmental toxins (6, 10). Coupled with CYP2E1, our laboratory has also shown the involvement of pattern recognition receptors following CYP2E1 activation that lead to innate immune activation (7). CYP2E1 induced metabolism of environmental toxins has also been shown to increase both circulating and hepatic leptin levels (8, 9). Leptin was found to activate Kupffer cells and innate immune mechanisms that contribute to NASH progression (8).

Though innate immune activation and TH1 cytokines have been found to escalate NASH progression several research reports also stress upon the involvement of hepatic T cells in the progression of NASH (11–14). Liver mononuclear cells, especially the CD4+ve, CD8+ve, NK and NKT cells are abundant in the liver and certain cells like NKT cells are deemed to be part of innate immune system. Distinct role of T cell subsets especially the cytotoxic T cells have been elucidated but there are scarce reports about their direct involvement in NASH progression (15). Though the involvement of T cell subsets in the fibrogenic process was discovered 25 years back, the literature remains scant in establishing the roles of T cells in NASH progression. This may be due to the paradox that several T cell cytokines like IFN-γ and IL-10 has been found to be aiding in resolution of fibrogenesis rather than accelerating it (15, 16). Especially striking are observations that CD8+ cytotoxic T lymphocytes contribute to the hepatic fibrogenesis. A role of CD8+ T cells as inducers of hepatic fibrosis was confirmed in a study in a CCl_4 model of hepatic fibrosis (15, 17). Beta glucosyl ceramide administration significantly reduced fibrosis and was associated with an altered distribution of CD8+ve lymphocytes and modulation of cytokine expression (17). The complex interplay between lymphocyte populations and expression of TH2 cytokines like IL-10 and IL-4 was recently underscored in a study where Copaxone, an immune modulator employed for the treatment of multiple sclerosis, was used in a toxic model of fibrogenesis (18). Copaxone had significant effects on the fibrogenesis pattern where it was associated with decreased CD8+ cells and serum IL-4 levels while NK cells, CD4(+) CD25(+) FoxP3(+) cells and serum IL-10 levels were increased (18). Interestingly, the

NIH-PA Author Manuscript

NIH-PA Author Manuscript

NIH-PA Author Manuscript

profibrogenic role of CD8+ T cells had already been hypothesized in a murine model of graft-versus-host disease several years before, on the basis that these cells were found as the main responsible of fibrosis (19).

The role of CD8+ Lymphocytes was also described in alcoholic liver disease. In alcoholic cirrhosis, significant reductions of CD4+ T cells correlated with severity of liver cirrhosis (20). Along these lines, a decreased CD4+ cells and a corresponding increase in CD8+ T cells were reported in chronic hepatitis C model (21). More importantly, a recent report suggested that hepatic stellate cells physically interact with lymphocytes in vivo (22). The activated state of hepatic stellate cells was upregulated by CD8+ T lymphocytes and in vitro experiments indicated that lymphocytes undergo phagocytosis within HSCs, a process prevented by integrin receptor blockade or irradiation of HSC. Thus, a direct pathway responsible for modulation of fibrogenesis by lymphocytes, and specifically CD8+ T cells, could be the end result of this important study (22).

Although there are studies indicating the role of CD8+ T cells in hepatic fibrosis, expression of other parallel markers on the CD8+ T cells and their role in hepatic fibrosis has never been studied especially those that will help in the progression of NASH. CD8+ T cells that express CD28 markers have been found in many chronic diseases including patients of alcoholism and other conditions where repeated antigenic stimulations are involved (23). It is established that upon chronic antigenic stimulation CD8+ CD28+ T cells rapidly lose their CD28 expression and become apoptotic (24). Strikingly the cells that enter a phase of senescence have higher expressions of CD57 on the CD8+ T cells (24). Together with the CD8+ and CD57+ expression these cells undergo rapid apoptosis and have short telomere length (23, 24). The presence of the CD8+CD57+ cells have been documented in non-viral infections, transplantation cases, chronic alcoholism and chronic pulmonary diseases that have immunosuppression as a major event(23–28). Chronic alcoholics with or without liver disease have very stable expressions of CD8+ CD57+ cells with the hepatocyte injury-associated antigenic exposure as a cause for the existence of these cells (27). Interestingly the study reports that the likely cause could be the chronic antigenic exposure resulting from acetaldehyde protein adducts (27, 29). It may be recalled that in free radical metabolism of toxins that aid in development of NASH, lipid peroxidation products also form adducts on proteins that can result in chronic antigenic stimulation (6, 9).

Another important mediator of hepatic fibrogenesis is the adipokine leptin which has been shown to activate the hepatic stellate cells and promote fibrogenesis (6, 30, 31). Importantly leptin also has a significant role in T cell proliferation (32). In a study published by Matiolli et al. it was found that in immature dendritic cells, leptin upregulates interleukin-12p70 production on CD40 stimulation and increases their capacity to stimulate activation of autologous CD8(+) T cells (33).

Thus in the light of the existing literature we hypothesized that upon metabolic oxidative stress, which is common following activation of CYP2E1 in a rodent model of environment-linked NASH, CD57+ expression in T cells play a crucial role in progression of the fibrogenesis. The hepatic fibrogenic mechanisms are mediated by leptin, an adipokine that is elevated following CYP2E1 activation and toxin exposure. We show that there is a huge increase in CD57 expression (70–90 fold) in the liver of mice exposed to BDCM and is down regulated in mice that lack T,B and NK cells. Further, mice with spontaneous knockout of leptin (OB/OB) have significant decrease in CD57 expression. Also important is the observation that CD57 was found mostly in CD8+ T cells and lack of T,B or NK cells had significantly reduced apoptosis, fibrogenesis and NASH progression.

NIH-PA Author Manuscript

NIH-PA Author Manuscript

NIH-PA Author Manuscript

Materials and Methods

Mouse model

Pathogen-free, custom, diet-induced obese (DIO) adult male mouse with a C57BL/6J background (Jackson Laboratories, Bar Harbor, Maine) was used as the model for toxin-induced non-alcoholic steatohepatitis (NASH). They were fed with a high fat diet (60% kcal) from 6 weeks to 16 weeks. All experiments were conducted at the completion of 16-weeks. The animals were housed one in each cage before any experimental use. Mice (C57BL/6J background) with CYP2E1 gene deletion (129/Sv-*Cyp2e1*^{tm1Gonz}/J, Jackson Laboratories) and mice (C57BL/6NTac background) with Pfp/Rag2 dual gene deletion (B6.129S6-*Rag2*^{tm1Fwa}*Prf1*^{tm1Clrk} N12, Taconic Farms Inc., Hudson, New York) were fed with high fat diet and treated identically to DIO mice. The four different kinds of mice that were used for experiments were: (i) diet-induced obese mouse (DIO), (ii) diet-induced obese mouse exposed to bromodichloromethane (DIO+BDCM), (iii) diet-induced obese mouse with CYP2E1 gene deletion and exposed to BDCM (CYP2E1 KO), (iv) diet-induced obese mouse with Pfp/Rag2 dual gene deletion and exposed to BDCM (Pfp/Rag2 dKO). Mice had *ad libitum* access to food and water and were housed in a temperature-controlled room at 23–24°C with a 12-hour light/dark cycle. All animals were treated in strict accordance with the NIH Guide for the Humane Care and Use of Laboratory Animals, and the experiments were approved by the institutional review board both at NIEHS and the University of South Carolina at Columbia, USA.

Induction of liver injury in mice

DIO mice or high-fat-fed gene-specific knockout mice at 16 weeks were administered bromodichloromethane (BDCM) obtained from Sigma Aldrich, St Louis, MO, at 1.0 mmole/kg, diluted in olive oil. The diluted BDCM were administered two doses per week for four weeks through the intra-peritoneal route. DIO mice treated with olive oil (diluent of BDCM) were used as vehicle-treated control. After completion of the treatment, mice of all study groups were sacrificed for liver tissue and serum for the further experiments.

Immunohistochemistry

Formalin-fixed, paraffin-embedded liver tissue from all the mouse groups were cut into 5 μm thick tissue sections. Each section was deparaffinized using standard protocol. Briefly, sections were incubated with xylene twice for 3 min, washed with xylene:ethanol (1:1) for 3 min and rehydrated through a series of ethanol (twice with 100 %, 95%, 70%, 50%), twice with distilled water and finally rinsed twice with phosphate buffered saline (PBS) (Sigma-Aldrich). Epitope retrieval of deparaffinized sections was carried out using epitope retrieval solution and steamer (IHC-world, Woodstock, MD) following manufacturer's protocol. The primary antibodies were (i) anti-4-hydroxynonenal, (ii) anti-3-nitrotyrosine, (iii) anti-CD57, (iv) anti-α-SMA and (v) anti-TGF-β. Primary antibodies were purchased from AbCam Inc. (Massachussetts, USA), and used in 1:250 dilutions. Antigen specific immunohistochemistry (IHC) were performed using Vectastain Elite ABC kit (Vector Laboratories, Inc. Burlingame, CA) following manufacturer's protocols. 3,3'Diaminobenzedine (DAB) (Sigma-Aldrich) were used as a chromogen substrate. Sections were counter-stained by Mayer's hematoxylin (Sigma-Aldrich). Washing with PBS (Sigma-Aldrich) was performed thrice between the steps. Sections were mounted in Simpo mount (GBI Labs, Mukilteo, WA) and observed under 20× oil objective.

Mitochondrial Nitrotyrosine assay

Mitochondrial protein extract was prepared using Mitochondrial Isolation kit (AbCam Inc. Massachussetts, USA) and following manufacturer's protocol. Standard ELISA was

NIH-PA Author Manuscript

NIH-PA Author Manuscript

NIH-PA Author Manuscript

performed to estimate the mitochondrial 3-nitrotyrosine. Briefly, high binding, round bottom 96-well ELISA plates were coated with 5μg/well of mitochondrial proteins and incubated at 4°C overnight. The wells were blocked with 5% non-fat milk in PBST for 1 h at RT. After washing with PBST anti-3-nitrotyrosine antibody (1:1000) were incubated for 2 h at RT. The plates were washed and incubated with species-specific anti-IgG conjugated with biotin (1:5000) for 1 h at RT. The plates were washed with PBST and incubated with streptavidin/HRP solution for 1 h at RT. Finally, plates were washed and developed with chemiluminescent ELISA substrate. Total luminescence was recorded using Synergy^{HT} microplate reader (BioTek, Winooski, VT).

Quantitative Real Time Polymerase Chain Reaction (qRTPCR)

Gene expression levels in tissue samples were measured by two step qRTPCR. Total RNA was extracted from liver tissue by homogenization in TRIzol reagent (Invitrogen, Carlsbad, CA) according to the manufacturer's instructions and purified with the use of RNeasy mini kit columns (Qiagen, Valencia, CA). Purified RNA (1μg) was converted to cDNA using iScript cDNA synthesis kit (Bio-rad, Hercules, CA) following the manufacturer's standard protocol. qRTPCR was performed with the gene specific primers using SsoAdvancedSYBR Green supermix (Bio-rad) and CFX96 thermal cycler (Bio-rad). Threshold Cycle (Ct) values for the selected genes were normalized against 18sRNA (internal control) values in the same sample. Each reaction was carried out in triplicates for each gene and for each tissue sample. DIO mouse liver sample was used as the control for comparison with all other liver samples in the toxin-induced NASH group. The relative fold change was calculated by the $2^{-\Delta\Delta Ct}$ method. The sequences for the primers used for Real time PCR are provided below in 5' to 3' orientation:

Gene	Primer sequence
CD57	Sense: GGGTCATCTCTGGGTCATCC Antisense: TGCCCCTCTGAAGAACCAAC
CD3	Sense: GGAACAAATGTTGCTTGTCTGG Antisense: TCTTGGCAAACAGCAGTCGTA
CD4	Sense: CACACACCTGTGCAAGAAGC Antisense: GCGTCTTCCCTTGAGTGACA
CD8	Sense: GCCCTTCTGCTGTCCTTGAT Antisense: TAGTTGTAGCTTCCTGGCGG
CD28	Sense: ATGTACCCTCCGCCTTACCT Antisense: CCACTGTCACTAGCAAGCCA
IL-2	Sense: GTGCTCCTTGTCAACAGCG Antisense: GGGGAGTTTCAGGTTCCTGTA
IL-1β	Sense: CCTCGGCCAAGACAGGTCGC Antisense: TGCCCATCAGAGGCAAGGAGGA
IFN-γ	Sense: TGCGGGGTTGTATCTGGGGGT Antisense: GCGCTGGCCCGGAGTGTAGA
FasL	Sense: GCAGCAGCCCATGAATTACC Antisense: AGATGAAGTGGCACTGCTGTCTAC
Bcl-2	Sense: TCTTTGAGTTCGGTGGGGTC Antisense: GCCCAGACTCATTCAACCAGA
Casp3	Sense: AGCTGGACTGTGGCATTGAG Antisense: CCACGACCCGTCCTTTGAAT
p53	Sense: CACGTACTCTCCTCCCCTCAAT Antisense: AACTGCACAGGGCACGTCTT

NIH-PA Author Manuscript

NIH-PA Author Manuscript

NIH-PA Author Manuscript

Gene	Primer sequence
Leptin	Sense: GAGACCCCTGTGTCGGTTC Antisense: CTGCGTGTGTGAAATGTCATTG

Immuno-fluorescence microscopy

Paraffin-embedded liver tissue from all the mouse groups were cut into 5 μm thick sections. Each section was deparaffinized using standard protocol. Epitope retrieval of deparaffinized sections was carried out using epitope retrieval solution and steamer (IHC-world, Woodstock, MD) following manufacturer's protocol. The primary antibodies (i) anti-CD3, (ii) anti-CD8, and (iii) anti-CD57 were purchased from AbCam Inc. (Massachussetts, USA), and used in 1:250 dilutions. Species-specific anti-IgG secondary antibody conjugated with Alexa Fluor 488 or with Alexa Fluor 633 (Invitrogen, California, USA) were used together. Sections were mounted in ProLong gold antifade reagent with DAPI. Images were taken under 20×/40× oil objectives using Olympus BX51 microscope.

Western blotting

30 mg of tissue from each liver sample was homogenized in 100 μl of RIPA buffer (Sigma Aldrich) with protease inhibitor (1×) (Pierce, Rockford, IL) using dounce homogenizer. The homogenate was centrifuged, the supernatant was diluted 1:5 and used for SDS PAGE and subjected to western blotting. Novex (Invitrogen, California, USA) 4–12% bis-tris gradient gel was used for SDS PAGE. Proteins were transferred to nitrocellulose membrane (i) using precut nitrocellulose/filter paper sandwiches (Bio-Rad Laboratories Inc., California, USA) and Trans – Blot Turbo transfer system (Bio-Rad) in case of low molecular weight proteins; and (ii) using wet transfer module from Invitrogen in case of high molecular weight proteins. 5% non-fat milk solution was used for blocking. Primary antibodies against caspase-3 and leptin (obtained from AbCam Inc.), FasL, p53 and Bcl2 (obtained from Santacruz Biotech) were used at recommended dilutions; and compatible HRP-conjugated secondary antibodies (from AbCam) were used. Pierce ECL Western Blotting substrate (Thermo Fisher Scientific Inc., Rockford, IL) was used as the chemiluminescent substrate. The blot was developed using BioMax MS Films and cassettes (with intensifying screen, Kodak). The images were subjected to densitometry analysis using LabImage 2006 Professional 1D gel analysis software from KAPLEAN Bioimaging Solutions, Liepzig, Germany.

TUNEL assay

Formalin-fixed, paraffin-embedded liver tissue from all the mouse groups were cut into 5 μm thick tissue sections. Each section was deparaffinized using the following protocol. Briefly, sections were incubated at 57°C for 5 min, with xylene twice for 3 min, rehydrated through a series of ethanol (twice with 100 %, 95%, 70%, 50%), twice with distilled water and finally rinsed twice with phosphate buffered saline (PBS) (Sigma-Aldrich). TUNEL staining to determine the number of apoptotic nuclei was done using TACS.XL Blue Label kit from Trevigen Inc., Gaithersburg, MD, following manufacturer's protocol. Nuclear Fast Red (Trevigen Inc.) was used as counterstain. All stained sections were mounted using toluene-based mounting medium (Trevigen Inc.) and imaged under 20× magnification.

Quantification of hepatic collagen content

Macro- and micro-vescicular collagen content in liver tissue was evaluated using morphometric analysis of Sirius red–stained liver sections. Each liver section (5 μm thick, paraffin-embedded) was deparaffinized and stained with Picro-Sirius red staining kit (IHC

NIH-PA Author Manuscript

NIH-PA Author Manuscript

NIH-PA Author Manuscript

World) and counterstained with Weigert's hematoxylin as per manufacturer's protocol. Collagen staining was quantitated in sections from all mice (magnification 10×; three fields from each section).

Statistical Analyses

All *in vivo* experiments were repeated three times with 3 mice per group (N=3; data from each group of three mice were pooled). All *in vitro* experiments were repeated three times, and the statistical analysis was carried out by analysis of variance (ANOVA) followed by the Bonferroni posthoc correction for intergroup comparisons. Quantitative data from Western blots as depicted by the relative intensity of the bands were analyzed by performing a student's t test. $P<0.05$ was considered statistically significant.

Results

CYP2E1 dependent metabolic oxidative stress following high fat diet feeding and environmental toxin exposure results in lipid peroxidation, tyrosyl radical formation and mitochondrial tyrosine nitration

Metabolic oxidative stress either from high fat diet alone, or through a second hit from environmental toxins, metabolized by CYP2E1, causes progression from steatosis to NASH(6, 34). To investigate the nature of metabolic oxidative stress following BDCM exposure in mice that were fed with a high fat diet, lipid peroxidation as measured by 4-hydroxynonenal (4-HNE) adducts in the liver were analyzed. Results indicated that DIO mice exposed to BDCM (DIO+BDCM) livers showed significantly increased 4-HNE adducts as compared to DIO mice and mice that had a deletion of the CYP2E1 gene, fed with a high fat diet and exposed to BDCM (CYP2E1 KO) (Fig. 1A and 1C) ($P<0.05$). CYP2E1 metabolism of BDCM causes protein radical formation and it has been found that the radical formation happens mostly at the tyrosine moiety. To identify the extent and nature of the tyrosyl radical formation, 3-nitrotyrosine immunoreactivity was assessed in DIO, DIO+BDCM and CYP2E1 KO groups. Results showed that 3-nitrotyrosine immunoreactivity was significantly increased in DIO+BDCM group as compared to both DIO and CYP2E1 KO group (Fig. 1B and 1D)($P<0.05$). Metabolic oxidative stress is also associated with mitochondrial generation of reactive oxygen species that disrupt normal functioning of the mitochondria (35). To assess the mitochondrial generation of protein radicals, tyrosine nitration, which can be a direct consequence of tyrosyl radical formation was analyzed by isolating mitochondrial counterpart from the livers of exposed groups. Results showed that mitochondrial 3-nitrotyrosine immunoreactivity as measured by a direct ELISA was significantly higher in DIO+BDCM group as compared to DIO and CYP2E1 KO groups (Fig. 1E)($P<0.05$).

Metabolic oxidative stress in progressive NASH causes T cell expression of CD57 that is CYP2E1 dependent

It has been reported that by controlling and modulating oxidative stress in the extracellular milieu might influence T cell signaling and activation (36). Further toxins can influence lipid peroxidation which in turn can give rise to T cell proliferation, especially 4-HNE adducts (37). To elucidate the T cell activation process in response to oxidative stress in DIO+BDCM, mRNA expressions of T cell markers and IL-2 expression was assessed. Results showed that CD57 (80 fold when compared to DIO mice) and pan T cell marker CD3 (20–25 fold) were significantly increased in DIO+BDCM group as compared to DIO, CYP2E1KO and Pfp/Rag2 gene deleted mice co exposed to high fat diet and BDCM (Pfp/Rag2 dKO) (Fig. 2A)($P<0.05$). To explore the nature of T cells that were activated following metabolic oxidative stress, mRNA expressions of CD4, CD8 and CD28 mRNA expressions were assessed. Results showed that CD8 rather than CD4 mRNA was significantly

NIH-PA Author Manuscript

NIH-PA Author Manuscript

NIH-PA Author Manuscript

expressed in DIO+BDCM group as compared to CYP2E1KO and Pfp/Rag2 dKO (Fig. 2A) ($P<0.05$). CD28 and CD4 mRNA expressions were only increased marginally in DIO +BDCM group. IL-2 which is a T cell cytokine and is the principle cytokine required for the T cell proliferation process was significantly elevated in DIO+BDCM group when compared to CYP2E1KO and Pfp/Rag2 dKO groups (Fig. 2A)($P<0.05$). Since mRNA expression of CD57, a marker expressed on a subclass of T cells that have a prominent role in T cell senescence, aging and apoptosis, we measured the CD57 protein and localization of this marker in the liver. Results showed that CD57 immunoreactivity as assessed by immunohistochemistry in liver slices, was high in DIO+BDCM group and the localization was markedly increased in Zone 3 and portal areas, when compared to CYP2E1KO and Pfp/Rag2 dKO groups (Fig. 2B). To explore the cell type for the expression of CD57, which carried immense significance in its role in the progression of NASH and its fibrotic pattern, and since the double knockout mice model (Pfp/Rag2) does not contain T, B and NK cells, it was essential for us to use co-localization analysis as a tool to analyze the cell type that contained the CD57 expression. Immuno-fluorescence revealed that CD3 and CD57 containing cells colocalized (Fig. 2C, viii) while there was a mismatch in localization of CD57/NK1.1 and CD57/CD22 cells (data not shown). CD3/CD57 colocalization was decreased in mice either containing a deletion of the CYP2E1 gene or the Pfp/Rag2 gene, suggesting that (a) the metabolic oxidative stress was responsible for the CD3 based expression of CD57 and (b) T cells were primarily responsible for increased expression of CD57 (Fig. 2C). Published literature indicates the important role of CD8+ve cytotoxic T cells that co-express CD57, in aging, apoptosis and many chronic diseases, mainly arising from successive antigenic stimulation (23, 24). Also there are prominent roles of this subclass of T cells in pulmonary fibrosis and in chronic alcoholic drinkers (27). To find the T cell subsets, mainly CD8+ve cytotoxic T cells that are primarily expressing the CD57 molecule, fluorescence imaging were performed at both low and high magnifications. Results indicated that CD8+ve T cells colocalized with CD57 molecules in DIO+BDCM group while no such colocalization was observed in CYP2E1KO or Pfp/Rag2 dKO groups (Fig. 2D), suggesting that the metabolic oxidative stress caused an increase in CD8+veCD57+ve T cells following exposure to high fat diet and BDCM.

CD8+veCD57+ve T cells produces pro-apoptotic cytokines, activate hepatic apoptosis, a process that is dependent on the presence of CYP2E1

Both T cell cytokines IL-1β and IFN-γ are reported to play major roles in the cellular apoptosis process, either through direct T cell mediated effects or through the inflammosome activation (38, 39). Since CD8+veCD57+ve cells are also reported to produce increased amounts of IL-1β and IFN-γ and FasL (CD95L) plays a major role in T cell mediated apoptosis, we estimated the mRNA expression of these mediators (24, 40, 41). Results showed that there was a significant increase in the mRNA levels of IL-1 β, IFN-γ and FasL in the DIO+BDCM group as compared to CYP2E1KO and Pfp/Rag2 dKO groups (Fig. 3A)($P<0.05$). To elucidate the effector downstream actions of CD8+ve CD57+ve T cells in NASH pathogenesis, apoptosis mechanisms of liver tissue was analyzed. mRNA analysis of Bcl-2, an important regulator of mitochondrial pathway of apoptosis, caspase-3, the terminal caspase and p53, a critical transcription factor for apoptosis, was performed. Results showed that Bcl-2 and p53 mRNA expressions were significantly elevated in DIO +BDCM group when compared to DIO, CYP2E1KO and Pfp/Rag2 dKO mice (Fig. 3B) ($P<0.05$). However there was no change in the levels of caspase-3 (Fig. 3B). Since the activation of terminal caspase (caspase-3) is brought about by the cleavage of caspase-3 into small peptides of low molecular weight, we performed western blot analysis of both caspase-3 and its cleaved isoforms. Results showed that DIO+BDCM group had both the larger and the smaller subunits of cleaved caspase-3 while DIO and Pfp/Rag2 dKO mice did not have the cleaved caspase-3 bands (Fig. 3C). CYP2E1 gene deleted mice that were co-

NIH-PA Author Manuscript

NIH-PA Author Manuscript

NIH-PA Author Manuscript

exposed to high fat diet and BDCM only had a larger cleaved subunit but the smaller cleaved subunit was inconspicuous (Fig. 3C and 3D). To estimate the morphological basis of apoptosis, TUNEL assay for liver slices from DIO, DIO+BDCM and the corresponding gene deleted livers were performed. Results showed that there was a significant increase in the TUNEL positive cells in the DIO+BDCM group (89%) as compared to DIO (48%) or CYP2E1 KO (12%) or Pfp/Rag2 dKO (10%) mice (Fig. 3E and 3F)($P<0.05$), suggesting that CD8+veCD57+cells might be responsible for apoptosis. Western Blot analysis of apoptotic proteins revealed that FasL, p53 and Bcl2 were increased in DIO+BDCM group while decreased in CYP2E1 KO and Pfp/Rag2 dKO groups respectively (Fig 3G).

Metabolic Oxidative stress-induced Leptin mediates CD57 expression on CD8+ve T cells and facilitates activation of this CD8+veCD57+ve phenotype in the liver of BDCM-treated DIO mice

CYP2E1 reductive metabolism is associated with increased leptin production in the liver and is found in increased concentration in circulation, higher than leptin resistant conditions of obesity (8). We have shown before that following CYP2E1 reductive metabolism of CCl_4 and BDCM, higher leptin concentrations are induced in the liver (9). Leptin mRNA expression were significantly high in DIO+BDCM group as compared to DIO group alone (Fig. 4A)($P<0.05$). Leptin protein levels as estimated by western blot analysis was also significantly higher in DIO+BDCM group when compared to DIO group alone (Fig. 4B). Our earlier results showed that metabolic oxidative stress significantly up-regulated CD57 protein on CD8+ve T cells accompanied by higher CD3 and CD8 T cells. To explore whether the increased T cell expression of CD57 was modulated by leptin, OB/OB mice that are spontaneous knockouts of leptin were used. Results showed that CD57, CD28, CD3, CD8 and IL2 mRNA expressions were significantly decreased in OB/OB mice coexposed with high fat diet and BDCM (Leptin KO) when compared to DIO+BDCM group (Fig. 4C) ($P<0.05$). The T cell cytokines (IFN-γ and IL-1β) and FasL which have a role in fibrogenesis and apoptosis and have been shown to be released following activation of CD8+veCD57+ve T cell phenotypes were significantly decreased in the Leptin KO mice when compared to DIO+BDCM group (Fig. 4D)($P<0.05$). CD57 protein levels as estimated by the CD57 immunoreactivity in liver slices was significantly decreased in Leptin KO mice when compared to DIO+BDCM (Fig. 4E and 4F)($P<0.05$). CD8+veCD57+ve colocalization was analyzed using fluorescence microscopy and results showed that leptin knockout mice had decreased colocalization events as compared to DIO+BDCM group (Fig. 4G) suggesting that leptin strongly mediates CD57 expression on CD8 Tcells and plays a role in their activation process. To prove that leptin mediation of the activation of CD8+veCD57+ve phenotype T cells contributed to NASH pathogenesis and apoptosis, liver slices from DIO +BDCM, Leptin KO and Pfp/Rag2 dKO mice-treated with high fat diet and BDCM were analyzed for fibrogenesis indicators α-SMA, TGF-β and collagen deposition (Picrosirius red staining). Results showed that α-SMA and TGF-β were significantly decreased in both Leptin KO and Pfp/Rag2 dKO groups as compared to DIO+BDCM group (Fig. 5A and 5B) ($P<0.05$). Picrosirius red staining for collagen was also decreased in Leptin KO and Pfp/ Rag2 dKO mice suggesting leptin-mediated CD8+CD57+ve T cell subsets might be modulated by the presence of leptin (Fig. 5C). Further to show that leptin also mediates the apoptotic process in the liver, a function which is associated with CD8+veCD57+ve T cells in chronic disease, TUNEL assay, mRNA expression analysis of apoptotic proteins and measurement of active caspase-3 were performed. Results showed that Leptin KO mice had significantly decreased TUNEL positive cells (Fig. 5D and 5E), Bcl-2 and p53 mRNA expressions as compared to DIO+BDCM group (Fig. 5F) ($P<0.05$). Results also showed that Leptin KO mice had significantly decreased active caspase-3 subunits as compared to DIO +BDCM group suggesting that leptin mediated the apoptotic effects of the CD8+veCD57+ve T cells (Fig. 5G)(band quantification not shown)($P<0.05$). Further a

NIH-PA Author Manuscript

NIH-PA Author Manuscript

NIH-PA Author Manuscript

detailed graphical representation of the proposed pathway of CD8+veCD57+ve T cell role in NASH pathogenesis is shown in Fig.6.

Discussion

Our study shows for the first time that CD57 expression on CD8+ve cells are increased following metabolic oxidative stress during NASH progression and this increased expression correlate well with increased hepatic apoptosis followed by development of NASH. We are not aware of any reports that indicate the involvement of CD57 in NASH progression and the novel finding that mostly CD8+ve cells carry the increased expression of CD57 augurs well for a new and unique pathway for the involvement of T cells in NASH Pathogenesis. Further, our studies also show that the increased CD57 levels and expression are mediated by leptin, which has a simultaneous role in the inflammatory pathways in NASH and the fibrogenesis that follows.

Our discovery of CD57+ve CD8+ve cells in rodent liver is in stark contrast to earlier reports where studies show that there are no CD8+ve CD57+ve T cells in rodents (42, 43). This may be due to an organ specific compartmentalization of these T cell subsets which were not observed earlier.

Our results are also significant in the findings that show that the CD57 expression was metabolic oxidative stress driven and was highly dependent on CYP2E1, a xenobiotic enzyme present in higher concentrations in the liver parenchymal cells. Few research reports show that controlling and modulating oxidative stress in the extra cellular milieu may influence T cell signaling and activation (36). T cells that undergo successive cell divisions as might happen initially during NASH progression may be subject to proliferative stress and/or oxidative stress as in the case here and reach replicative senescence (23). It is important to consider at this point that CD57 expression has been found to increase on CD8+ve T cells in cases of repeated antigenic stimulation with a progressive loss of CD28 (23). The consequence of a metabolic oxidative stress mediated higher population of CD57 expressing CD8+ve T cells, with a simultaneous drop in CD28 can be two fold. The rise in CD57 expression can pave way for higher cytokine production and also more apoptosis as seen in our studies. Though our studies do not confirm whether the same T cells undergo apoptosis but there is a definite correlation between higher CD57 expression and hepatic apoptosis in our studies. The results are in agreement with another study in alcoholic drinkers that showed cell death in hepatic parenchyma following a stable expansion of CD8+ve CD57+ve cells (27). We used Pfp/Rag2 dKO mice to establish the role of liver mononuclear cells, especially B cells, T cells and NK cells which might have the expression of CD57. The results showed that CD57 expression was significantly decreased in these mice accompanied by decreased T cell cytokines IL-1β, IL-2, IFN-γ and CD95L (FasL). Interestingly there are contrasting reports about the involvement of IFN-γ in fibrosis, where the role of IFN-γ in causing liver fibrosis is skewed (11). There are many in vivo and in vitro studies that report the proinflammatory actions of IFN-γ and work towards resolution of fibrosis but studies that involve choline deficient and ethionine supplemented diets showed IFN-γ administration increased progenitor cell proliferation, caused increased inflammation and fibrosis (44–46). In our studies where we see an increased IFN-γ release in the liver might be a consequence of higher expression of CD57+ve cells on CD8+ve cytotoxic T lymphocytes that are a consequence of the higher metabolic oxidative stress in this model. The higher IFN-γ production in these cells is supported by another study which found increased production of this cytokine that correlated well with higher number of CD8+ve highCD28-veCD57+ subpopulation (47). Our studies further showed that there was also a significant reduction of liver apoptosis in these mice. However, at this point the use of Pfp/Rag2 dKO mice restricted us from inferring conclusively that the CD57 expression was

NIH-PA Author Manuscript

NIH-PA Author Manuscript

NIH-PA Author Manuscript

specifically more in CD8+ve cytotoxic T cells since we did not use mice that were specifically deficient in CD8+ T lymphocytes. To prove that the CD8+ve cells were mainly expressing higher CD57+ve cells, fluroscence microscopy was used. Using dual dye labeling and colocalization analysis it was revealed that CD57 expression was mainly in CD8+ve cells. Future studies are planned to elucidate more concerted roles of CD8+ve CD57+ve cells in an in vitro culture system using isolated liver specific mononuclear cells co-exposed to the environmental toxin and adipokine leptin. Following our observation that CD8+ve T cells had higher expression of CD57 and they might play a role in the fibrogenesis during NASH progression and since a role of CD8+ve cells in inducing fibrogenesis in a toxin model of liver fibrosis have been reported earlier (15), we explored the role of leptin-CD8 - axis in mediating the higher expression of CD57 on CD8+ve cells. It is reported that CD8+ve cells can up-regulate the activated state of hepatic stellate cells and so does leptin, which has a direct role in activating hepatic stellate cells (22, 48). Adipokine leptin is a 16kd protein with established roles in stellate cell activation, Kupffer cell activation, proinflammatory cytokine production and fibrogenesis in NASH (49). Leptin also has a significant role in T cell proliferation including activation of CD8+ve T cells (32). A study by Mattioli B et al found that leptin up-regulates interleukin-12p70 production on CD40 stimulation and, more importantly, increases their capacity to stimulate activation of autologous CD8(+) T cells (33). Metabolic oxidative stress following environmental toxin exposures like CCl_4 and BDCM caused increased levels of serum and hepatic leptin (8, 9). In the present study we also show increased leptin mRNA and protein in DIO+BDCM group, data that is consistent with our previous published reports. High leptin in our model of NASH, coupled with increased metabolic oxidative stress might lead to higher expression of CD57. This is also supported by the fact that OB/OB mice have less CD57 expression. Further, our observations show that OB/OB mice administered BDCM had significantly decreased CD57 expression on CD8+ve cells, decreased T cell cytokine levels and reduced apoptosis. The same mice were also protected from liver fibrosis and NASH progression. However the set of data that is shown does not directly outline the mechanisms of leptin induced CD57 expression on CD+ve T cells, nor does it clearly show how downstream leptin signaling might increase CD57 expression of CD8+ve cells. Future research can be directed towards exploring the mechanisms of leptin in immunosuppression and T cell senescence in NASH.

Taken together, the present study identifies for the first time that CD57 protein is increased in NASH progression and is primarily expressed on CD8+ve T cells. Further the metabolic oxidative stress dependent CD57 expression contributes to T cell cytokine increase, apoptosis and fibrogenesis in NASH, a process that is mediated by adipokine leptin (Fig. 6). This novel discovery of a more than 70–80 fold increase in CD57 in NASH livers makes this molecule to be an ideal biomarker for NASH pathogenesis.

Acknowledgments

The authors gratefully acknowledge the technical services of Benny Davidson at the IRF, University of South Carolina, School of Medicine. We also thank Dr David C. Volz for use of the BX51 fluorescence microscope, the Instrumentation resource facility (IRF) at the University of South Carolina School of Medicine for equipment usage and consulting services. This work has been supported by NIH pathway to Independence Award (4R00ES019875-02 to Saurabh Chatterjee), NIH R01(R01DK053792 to Anna Mae Diehl) and the Intramural Research Program of the National Institutes of Health and the National Institute of Environmental Health Sciences.

References

1. Nascimbeni F, Pais R, Bellentani S, Day CP, Ratziu V, Loria P, et al. From NAFLD in clinical practice to answers from guidelines. J Hepatol. 2013 Epub 2013/06/12. PubMed PMID: 23751754.

NIH-PA Author Manuscript

NIH-PA Author Manuscript

NIH-PA Author Manuscript

2. Fan JG. Epidemiology of alcoholic and nonalcoholic fatty liver disease in China. Journal of gastroenterology and hepatology. 2013; 28(Suppl 1):11–17. Epub 2013/07/24. PubMed PMID: 23855290. [PubMed: 23855290]

3. Fan JG, Farrell GC. Epidemiology of non-alcoholic fatty liver disease in China. J Hepatol. 2009; 50(1):204–210. Epub 2008/11/19. PubMed PMID: 19014878. [PubMed: 19014878]

4. Fan JG, Peng YD. Metabolic syndrome and non-alcoholic fatty liver disease: Asian definitions and Asian studies. Hepatobiliary & pancreatic diseases international : HBPD INT. 2007; 6(6):572–578. Epub 2007/12/19. PubMed PMID: 18086620. [PubMed: 18086620]

5. Wahlang B, Beier JI, Clair HB, Bellis-Jones HJ, Falkner KC, McClain CJ, et al. Toxicant-associated steatohepatitis. Toxicologic pathology. 2013; 41(2):343–360. Epub 2012/12/25. PubMed PMID: 23262638. [PubMed: 23262638]

6. Seth RK, Kumar A, Das S, Kadiiska MB, Michelotti G, Diehl AM, et al. Environmental toxin-linked nonalcoholic steatohepatitis and hepatic metabolic reprogramming in obese mice. Toxicological sciences : an official journal of the Society of Toxicology. 2013 Epub 2013/05/04. PubMed PMID: 23640861.

7. Chatterjee S, Rana R, Corbett J, Kadiiska MB, Goldstein J, Mason RP. P2×7 receptor-NADPH oxidase axis mediates protein radical formation and Kupffer cell activation in carbon tetrachloride-mediated steatohepatitis in obese mice. Free Radic Biol Med. 2012; 52(9):1666–1679. Epub 2012/02/22. PubMed PMID: 22343416; PubMed Central PMCID: PMCPMC3341527. [PubMed: 22343416]

8. Chatterjee S, Ganini D, Tokar EJ, Kumar A, Das S, Corbett J, et al. Leptin is key to peroxynitrite-mediated oxidative stress and Kupffer cell activation in experimental nonalcoholic steatohepatitis. J Hepatol. 2012 Epub 2012/12/05. PubMed PMID: 23207144.

9. Das S, Kumar A, Seth RK, Tokar EJ, Kadiiska MB, Waalkes MP, et al. Proinflammatory adipokine leptin mediates disinfection byproduct bromodichloromethane-induced early steatohepatitic injury in obesity. Toxicology and applied pharmacology. 2013 Epub 2013/02/27. PubMed PMID: 23438451.

10. Abdelmegeed MA, Banerjee A, Yoo SH, Jang S, Gonzalez FJ, Song BJ. Critical role of cytochrome P450 2E1 (CYP2E1) in the development of high fat-induced nonalcoholic steatohepatitis. J Hepatol. 2012; 57(4):860–866. Epub 2012/06/07. PubMed PMID: 22668639; PubMed Central PMCID: PMCPMC3445664. [PubMed: 22668639]

11. Marra F, Aleffi S, Galastri S, Provenzano A. Mononuclear cells in liver fibrosis. Seminars in immunopathology. 2009; 31(3):345–358. Epub 2009/06/18. PubMed PMID: 19533130. [PubMed: 19533130]

12. Smedsrod B, De Bleser PJ, Braet F, Lovisetti P, Vanderkerken K, Wisse E, et al. Cell biology of liver endothelial and Kupffer cells. Gut. 1994; 35(11):1509–1516. Epub 1994/11/01. PubMed PMID: 7828963; PubMed Central PMCID: PMCPMC1375602. [PubMed: 7828963]

13. Imamura M, Ogawa T, Sasaguri Y, Chayama K, Ueno H. Suppression of macrophage infiltration inhibits activation of hepatic stellate cells and liver fibrogenesis in rats. Gastroenterology. 2005; 128(1):138–146. Epub 2005/01/06. PubMed PMID: 15633130. [PubMed: 15633130]

14. Casini A, Ricci OE, Paoletti F, Surrenti C. Immune mechanisms for hepatic fibrogenesis. T-lymphocyte-mediated stimulation of fibroblast collagen production in chronic active hepatitis. Liver. 1985; 5(3):134–141. Epub 1985/06/01. PubMed PMID: 3876501. [PubMed: 3876501]

15. Safadi R, Ohta M, Alvarez CE, Fiel MI, Bansal M, Mehal WZ, et al. Immune stimulation of hepatic fibrogenesis by CD8 cells and attenuation by transgenic interleukin-10 from hepatocytes. Gastroenterology. 2004; 127(3):870–882. Epub 2004/09/14. PubMed PMID: 15362042. [PubMed: 15362042]

16. Shi Z, Wakil AE, Rockey DC. Strain-specific differences in mouse hepatic wound healing are mediated by divergent T helper cytokine responses. Proceedings of the National Academy of Sciences of the United States of America. 1997; 94(20):10663–10668. Epub 1997/10/06. PubMed PMID: 9380692; PubMed Central PMCID: PMCPMC23440. [PubMed: 9380692]

17. Safadi R, Zigmond E, Pappo O, Shalev Z, Ilan Y. Amelioration of hepatic fibrosis via beta-glucosylceramide-mediated immune modulation is associated with altered CD8 and NKT lymphocyte distribution. International immunology. 2007; 19(8):1021–1029. Epub 2007/08/19. PubMed PMID: 17698563. [PubMed: 17698563]

NIH-PA Author Manuscript

NIH-PA Author Manuscript

NIH-PA Author Manuscript

18. Horani A, Muhanna N, Pappo O, Melhem A, Alvarez CE, Doron S, et al. Beneficial effect of glatiramer acetate (Copaxone) on immune modulation of experimental hepatic fibrosis. American journal of physiology Gastrointestinal and liver physiology. 2007; 292(2):G628–G638. Epub 2006/10/14. PubMed PMID: 17038628. [PubMed: 17038628]
19. Inada S, Suzuki K, Kimura T, Hayashi A, Narita T, Yui R, et al. Concentric fibrosis and cellular infiltration around bile ducts induced by graft-versus-host reaction in mice: a role of CD8+ cells. Autoimmunity. 1995; 22(3):163–171. Epub 1995/01/01. PubMed PMID: 8734570. [PubMed: 8734570]
20. Lombardo L, Capaldi A, Poccardi G, Vineis P. Peripheral blood CD3 and CD4 T-lymphocyte reduction correlates with severity of liver cirrhosis. International journal of clinical & laboratory research. 1995; 25(3):153–156. Epub 1995/01/01. PubMed PMID: 8562979. [PubMed: 8562979]
21. Panasiuk A, Prokopowicz D, Zak J, Wysocka J. Peripheral blood T, B, and NK cells in relation to histological hepatitis activity and fibrosis stage in chronic hepatitis C. Hepato-gastroenterology. 2003; 50(49):178–182. Epub 2003/03/13. PubMed PMID: 12630018. [PubMed: 12630018]
22. Muhanna N, Doron S, Wald O, Horani A, Eid A, Pappo O, et al. Activation of hepatic stellate cells after phagocytosis of lymphocytes: A novel pathway of fibrogenesis. Hepatology. 2008; 48(3): 963–977. Epub 2008/08/30. PubMed PMID: 18726940; PubMed Central PMCID: PMCPMC2880478. [PubMed: 18726940]
23. Strioga M, Pasukoniene V, Characiejus D. CD8+ CD28− and CD8+ CD57+ T cells and their role in health and disease. Immunology. 2011; 134(1):17–32. Epub 2011/06/30. PubMed PMID: 21711350; PubMed Central PMCID: PMCPMC3173691. [PubMed: 21711350]
24. Brenchley JM, Karandikar NJ, Betts MR, Ambrozak DR, Hill BJ, Crotty LE, et al. Expression of CD57 defines replicative senescence and antigen-induced apoptotic death of CD8+ T cells. Blood. 2003; 101(7):2711–2720. Epub 2002/11/16. PubMed PMID: 12433688. [PubMed: 12433688]
25. Sada-Ovalle I, Torre-Bouscoulet L, Valdez-Vazquez R, Martinez-Cairo S, Zenteno E, Lascurain R. Characterization of a cytotoxic CD57+ T cell subset from patients with pulmonary tuberculosis. Clinical immunology (Orlando, Fla). 2006; 121(3):314–323. Epub 2006/10/13. PubMed PMID: 17035093.
26. Frassanito MA, Silvestris F, Cafforio P, Dammacco F. CD8+/CD57 cells and apoptosis suppress T-cell functions in multiple myeloma. British journal of haematology. 1998; 100(3):469–477. Epub 1998/03/21. PubMed PMID: 9504628. [PubMed: 9504628]
27. Song K, Coleman RA, Alber C, Ballas ZK, Waldschmidt TJ, Mortari F, et al. TH1 cytokine response of CD57+ T-cell subsets in healthy controls and patients with alcoholic liver disease. Alcohol (Fayetteville, NY). 2001; 24(3):155–167. Epub 2001/09/15. PubMed PMID: 11557301.
28. Sharma G, Hanania NA, Shim YM. The aging immune system and its relationship to the development of chronic obstructive pulmonary disease. Proceedings of the American Thoracic Society. 2009; 6(7):573–580. Epub 2009/11/26. PubMed PMID: 19934352. [PubMed: 19934352]
29. Arosa FA. CD8+CD28− T cells: certainties and uncertainties of a prevalent human T-cell subset. Immunology and cell biology. 2002; 80(1):1–13. Epub 2002/03/01. PubMed PMID: 11869357. [PubMed: 11869357]
30. Ikejima K, Takei Y, Honda H, Hirose M, Yoshikawa M, Zhang YJ, et al. Leptin receptor-mediated signaling regulates hepatic fibrogenesis and remodeling of extracellular matrix in the rat. Gastroenterology. 2002; 122(5):1399–1410. Epub 2002/05/02. PubMed PMID: 11984526. [PubMed: 11984526]
31. Wang J, Leclercq I, Brymora JM, Xu N, Ramezani-Moghadam M, London RM, et al. Kupffer cells mediate leptin-induced liver fibrosis. Gastroenterology. 2009; 137(2):713–723. Epub 2009/04/21. PubMed PMID: 19375424; PubMed Central PMCID: PMCPMC2757122. [PubMed: 19375424]
32. Matarese G, Moschos S, Mantzoros CS. Leptin in immunology. J Immunol. 2005; 174(6):3137–3142. Epub 2005/03/08. PubMed PMID: 15749839. [PubMed: 15749839]
33. Mattioli B, Straface E, Matarrese P, Quaranta MG, Giordani L, Malorni W, et al. Leptin as an immunological adjuvant: enhanced migratory and CD8+ T cell stimulatory capacity of human dendritic cells exposed to leptin. FASEB journal : official publication of the Federation of American Societies for Experimental Biology. 2008; 22(6):2012–2022. Epub 2008/01/26. PubMed PMID: 18218920. [PubMed: 18218920]

NIH-PA Author Manuscript

NIH-PA Author Manuscript

NIH-PA Author Manuscript

34. Mendelson KG, Contois LR, Tevosian SG, Davis RJ, Paulson KE. Independent regulation of JNK/p38 mitogen-activated protein kinases by metabolic oxidative stress in the liver. Proceedings of the National Academy of Sciences of the United States of America. 1996; 93(23):12908–12913. Epub 1996/11/12. PubMed PMID: 8917518; PubMed Central PMCID: PMCPMC24019. [PubMed: 8917518]
35. Morris EM, Rector RS, Thyfault JP, Ibdah JA. Mitochondria and redox signaling in steatohepatitis. Antioxid Redox Signal. 2011; 15(2):485–504. Epub 2010/12/07. PubMed PMID: 21128703; PubMed Central PMCID: PMCPMC3118705. [PubMed: 21128703]
36. Larbi A, Kempf J, Pawelec G. Oxidative stress modulation and T cell activation. Experimental gerontology. 2007; 42(9):852–858. Epub 2007/07/03. PubMed PMID: 17604927. [PubMed: 17604927]
37. Wang G, Konig R, Ansari GA, Khan MF. Lipid peroxidation-derived aldehyde-protein adducts contribute to trichloroethene-mediated autoimmunity via activation of CD4+ T cells. Free Radic Biol Med. 2008; 44(7):1475–1482. Epub 2008/02/13. PubMed PMID: 18267128; PubMed Central PMCID: PMCPMC2440665. [PubMed: 18267128]
38. Chawla-Sarkar M, Lindner DJ, Liu YF, Williams BR, Sen GC, Silverman RH, et al. Apoptosis and interferons: role of interferon-stimulated genes as mediators of apoptosis. Apoptosis : an international journal on programmed cell death. 2003; 8(3):237–249. Epub 2003/05/27. PubMed PMID: 12766484. [PubMed: 12766484]
39. Csak T, Ganz M, Pespisa J, Kodys K, Dolganiuc A, Szabo G. Fatty acid and endotoxin activate inflammasomes in mouse hepatocytes that release danger signals to stimulate immune cells. Hepatology. 2011; 54(1):133–144. Epub 2011/04/14. PubMed PMID: 21488066. [PubMed: 21488066]
40. Borthwick NJ, Lowdell M, Salmon M, Akbar AN. Loss of CD28 expression on CD8(+) T cells is induced by IL-2 receptor gamma chain signalling cytokines and type I IFN, and increases susceptibility to activation-induced apoptosis. International immunology. 2000; 12(7):1005–1013. Epub 2000/07/06. PubMed PMID: 10882412. [PubMed: 10882412]
41. Wood KL, Twigg HL 3rd, Doseff AI. Dysregulation of CD8+ lymphocyte apoptosis, chronic disease, and immune regulation. Frontiers in bioscience : a journal and virtual library. 2009; 14:3771–3781. Epub 2009/03/11. PubMed PMID: 19273309; PubMed Central PMCID: PMCPMC2740383.
42. Vallejo AN. CD28 extinction in human T cells: altered functions and the program of T-cell senescence. Immunological reviews. 2005; 205:158–169. Epub 2005/05/11. PubMed PMID: 15882352. [PubMed: 15882352]
43. Weng NP, Akbar AN, Goronzy J. CD28(−) T cells: their role in the age-associated decline of immune function. Trends in immunology. 2009; 30(7):306–312. Epub 2009/06/23. PubMed PMID: 19540809; PubMed Central PMCID: PMCPMC2801888. [PubMed: 19540809]
44. Czaja MJ, Weiner FR, Takahashi S, Giambrone MA, van der Meide PH, Schellekens H, et al. Gamma-interferon treatment inhibits collagen deposition in murine schistosomiasis. Hepatology. 1989; 10(5):795–800. Epub 1989/11/01. PubMed PMID: 2509321. [PubMed: 2509321]
45. Baroni GS, D'Ambrosio L, Curto P, Casini A, Mancini R, Jezequel AM, et al. Interferon gamma decreases hepatic stellate cell activation and extracellular matrix deposition in rat liver fibrosis. Hepatology. 1996; 23(5):1189–1199. Epub 1996/05/01. PubMed PMID: 8621153. [PubMed: 8621153]
46. Knight B, Lim R, Yeoh GC, Olynyk JK. Interferon-gamma exacerbates liver damage, the hepatic progenitor cell response and fibrosis in a mouse model of chronic liver injury. J Hepatol. 2007; 47(6):826–833. Epub 2007/10/10. PubMed PMID: 17923165. [PubMed: 17923165]
47. Bandres E, Merino J, Vazquez B, Inoges S, Moreno C, Subira ML, et al. The increase of IFN-gamma production through aging correlates with the expanded CD8(+high)CD28(−)CD57(+) subpopulation. Clinical immunology (Orlando, Fla). 2000; 96(3):230–235. Epub 2000/08/31. PubMed PMID: 10964541.
48. Saxena NK, Titus MA, Ding X, Floyd J, Srinivasan S, Sitaraman SV, et al. Leptin as a novel profibrogenic cytokine in hepatic stellate cells: mitogenesis and inhibition of apoptosis mediated by extracellular regulated kinase (Erk) and Akt phosphorylation. FASEB journal : official publication of the Federation of American Societies for Experimental Biology. 2004; 18(13):

NIH-PA Author Manuscript

NIH-PA Author Manuscript

NIH-PA Author Manuscript

1612–1614. Epub 2004/08/21. PubMed PMID: 15319373; PubMed Central PMCID: PMCPMC2924993. [PubMed: 15319373]

49. Kamada Y, Takehara T, Hayashi N. Adipocytokines and liver disease. Journal of gastroenterology. 2008; 43(11):811–822. Epub 2008/11/18. PubMed PMID: 19012034. [PubMed: 19012034]

NIH-PA Author Manuscript

NIH-PA Author Manuscript

NIH-PA Author Manuscript

Highlights

1. Metabolic oxidative stress caused increased levels of hepatic CD57, a marker of peripheral blood lymphocytes including NKT cells.
2. CD8+CD57+ cytotoxic T cells but not CD4+CD57+ cells were significantly decreased in mice lacking CYP2E1 and leptin.
3. There was a significant increase in the levels of T cell cytokines IL-2, IL-1β, IFN-γ in bromodichloromethane exposed DIO mice but not in mice that lacked CYP2E1, leptin or T and B cells.
4. Apoptosis as evidenced by TUNEL assay and levels of cleaved caspase-3 was significantly lower in leptin and Pfp/Rag2 KO mice and highly correlated with protection from NASH.
5. Leptin mediated CD8+CD57+ T cells play an important role in the development of NASH and also provides a novel insight of immune dysregulation and may be a key biomarker in NASH.

NIH-PA Author Manuscript
NIH-PA Author Manuscript
NIH-PA Author Manuscript

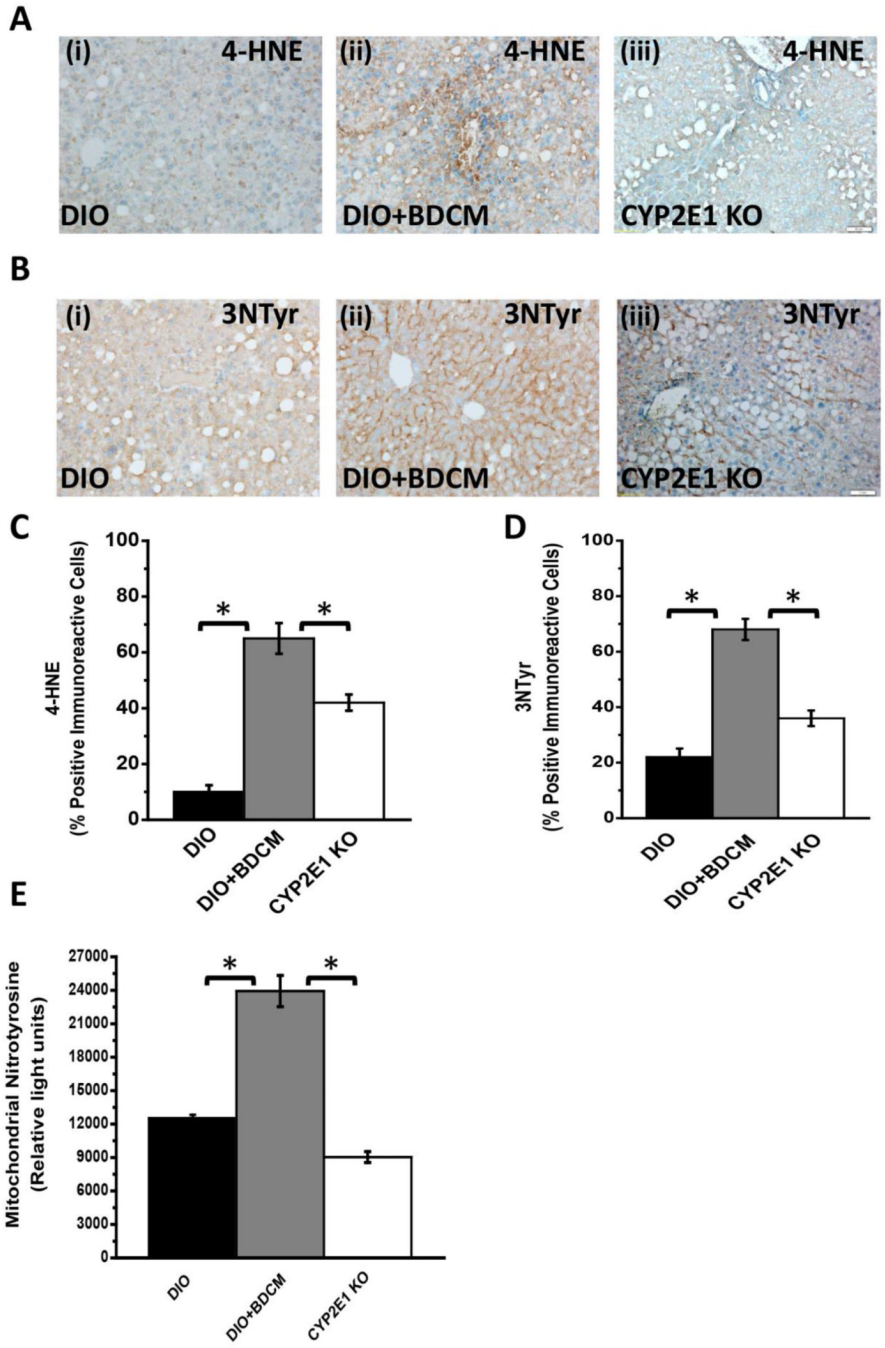

Fig.1.

A(i)–(iii). 4-Hydroxynonenal (4-HNE, a marker for lipid peroxidation) immunoreactivity as shown by immunohistochemistry in liver slices from diet-induced obese mouse (DIO), diet-induced obese mouse exposed to bromodichloromethane (DIO+BDCM), and diet-induced obese mouse with CYP2E1 gene deletion and exposed to bromodichloromethane (CYP2E1 KO) respectively. Images were taken in 20×. B (i)–(iii). 3-Nitrotyrosine (3NTyr, a marker for protein nitrosylation) immunoreactivity as shown by immunohistochemistry in liver slices from DIO, DIO+BDCM and CYP2E1 KO groups respectively. Images were taken in 20×. C. Percentage of 4-HNE positive immunoreactive cells (obtained by morphometry done on images from three separate microscopic fields) in DIO, DIO+BDCM and CYP2E1

KO groups (* P<0.05). D. Percentage of 3NTyr positive immunoreactive cells (obtained by morphometry done on images from three separate microscopic fields) in DIO, DIO+BDCM and CYP2E1 KO groups (* P<0.05). E. Quantification of mitochondrial nitrotyrosine levels (in relative light units), as determined by ELISA in DIO, DIO+BDCM and CYP2E1 KO groups (* P<0.05).

NIH-PA Author Manuscript
NIH-PA Author Manuscript
NIH-PA Author Manuscript

NIH-PA Author Manuscript
NIH-PA Author Manuscript
NIH-PA Author Manuscript

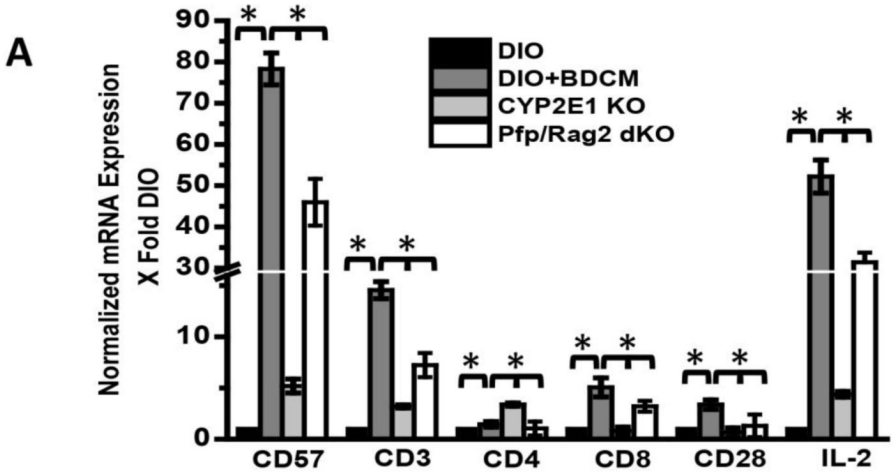

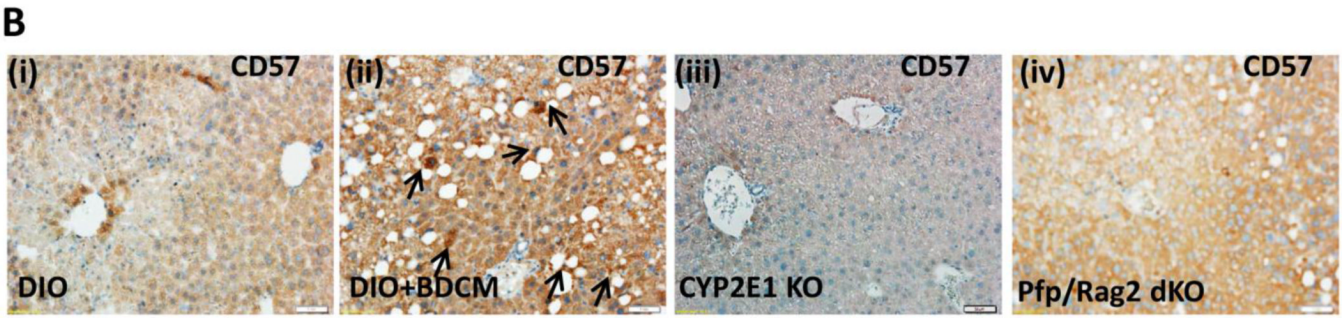

NIH-PA Author Manuscript
NIH-PA Author Manuscript
NIH-PA Author Manuscript

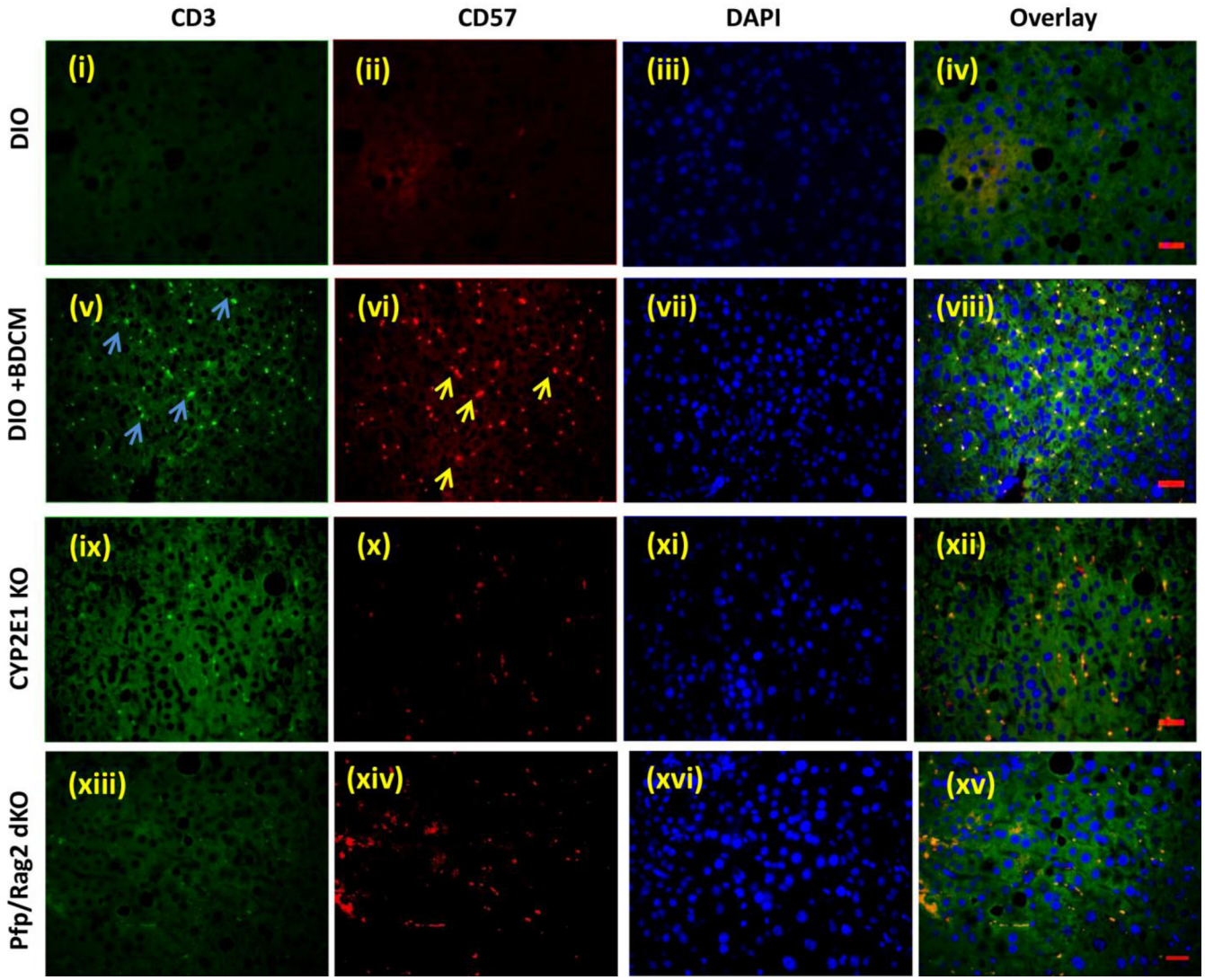

NIH-PA Author Manuscript
NIH-PA Author Manuscript
NIH-PA Author Manuscript

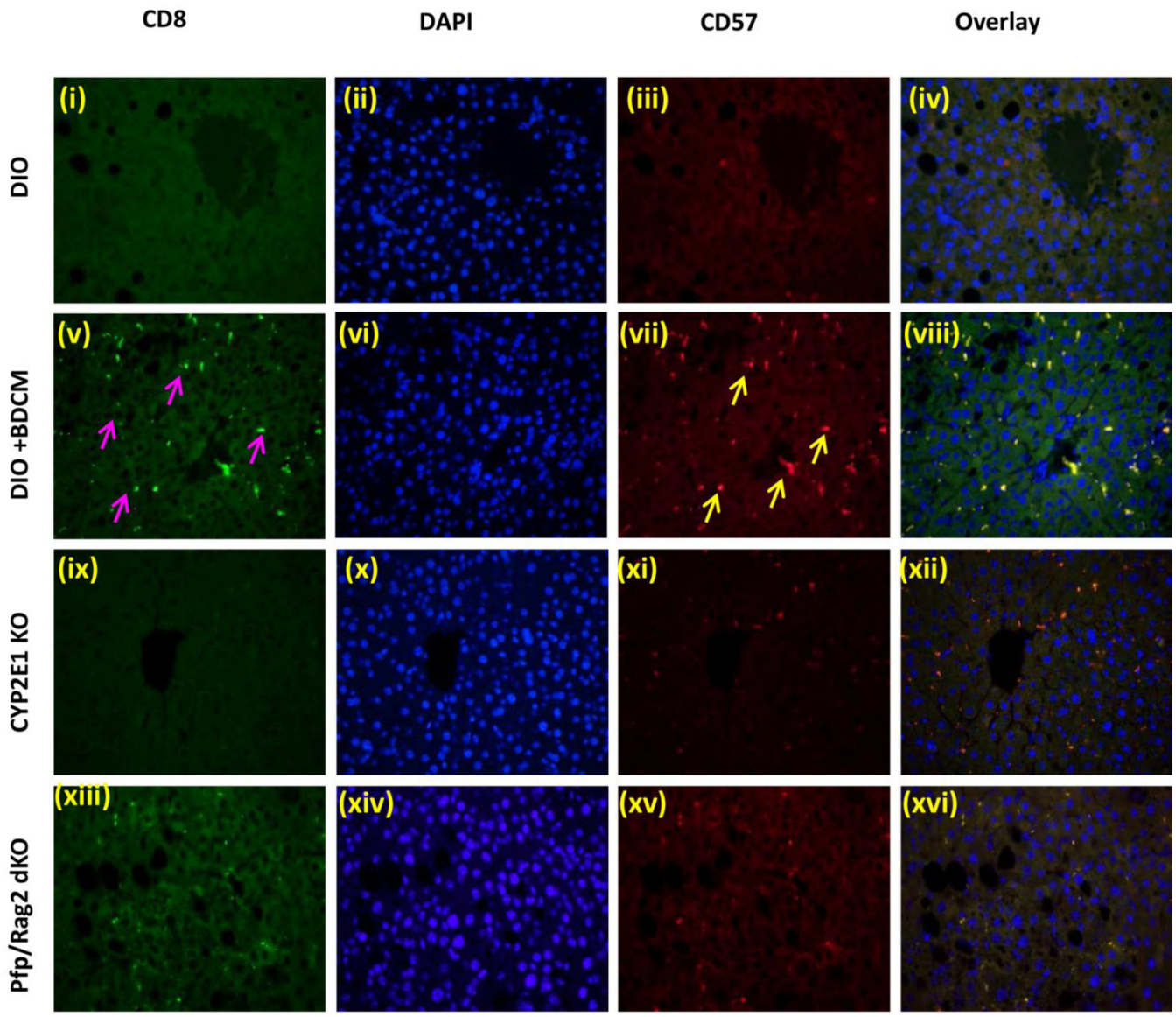

Fig.2.

A. mRNA expressions of CD57, CD3, CD4, CD8, CD28 and IL-2 from liver homogenates of diet-induced obese mouse (DIO), diet-induced obese mouse exposed to bromodichloromethane (DIO+BDCM), diet-induced obese mouse with CYP2E1 gene deletion and exposed to bromodichloromethane (CYP2E1 KO), and diet-induced obese mouse with Pfp/Rag2 dual gene deletion and exposed to bromodichloromethane (Pfp/Rag2 dKO). mRNA expressions had been assessed by quantitative real-time PCR (qRTPCR) and expressions in DIO+BDCM, CYP2E1 KO and Pfp/Rag2 dKO groups were normalized against mRNA expression in DIO group (* $P<0.05$). B (i)–(iv). CD57 immunoreactivity as shown by immunohistochemistry in liver slices from DIO, DIO+BDCM, CYP2E1 KO and Pfp/Rag2 dKO groups respectively. Images were taken in 20×. C. Immunofluorescence images for co-localization of CD57 (red) and CD3 (green) from liver sections of DIO [(i)–(iv)], DIO+BDCM [(v)–(viii)], CYP2E1 KO [(ix)–(xii)] and Pfp/Rag2 dKO [(xiii)–(xvi)] groups. The images in the overlay panel on the extreme right depict co-localizations of CD57 and CD3 as revealed by the yellow regions. The localizations of CD3 and CD57 are

shown by blue and yellow arrows respectively. Images were taken in 40× magnification. D. Immunofluorescence laser scanning images for co-localization of CD57 (red) and CD8 (green) from liver sections of DIO [(i)–(iv)], DIO+BDCM [(v)–(viii)], CYP2E1 KO [(ix)–(xii)] and Pfp/Rag2 dKO [(xiii)–(xvi)] groups. The images in the overlay panel on the extreme right depict co-localizations of CD57 and CD8 as revealed by the yellow regions. Images were taken in 40× magnification. The localizations of CD8 and CD57 are shown by pink and yellow arrows respectively.

NIH-PA Author Manuscript
NIH-PA Author Manuscript
NIH-PA Author Manuscript

NIH-PA Author Manuscript
NIH-PA Author Manuscript
NIH-PA Author Manuscript

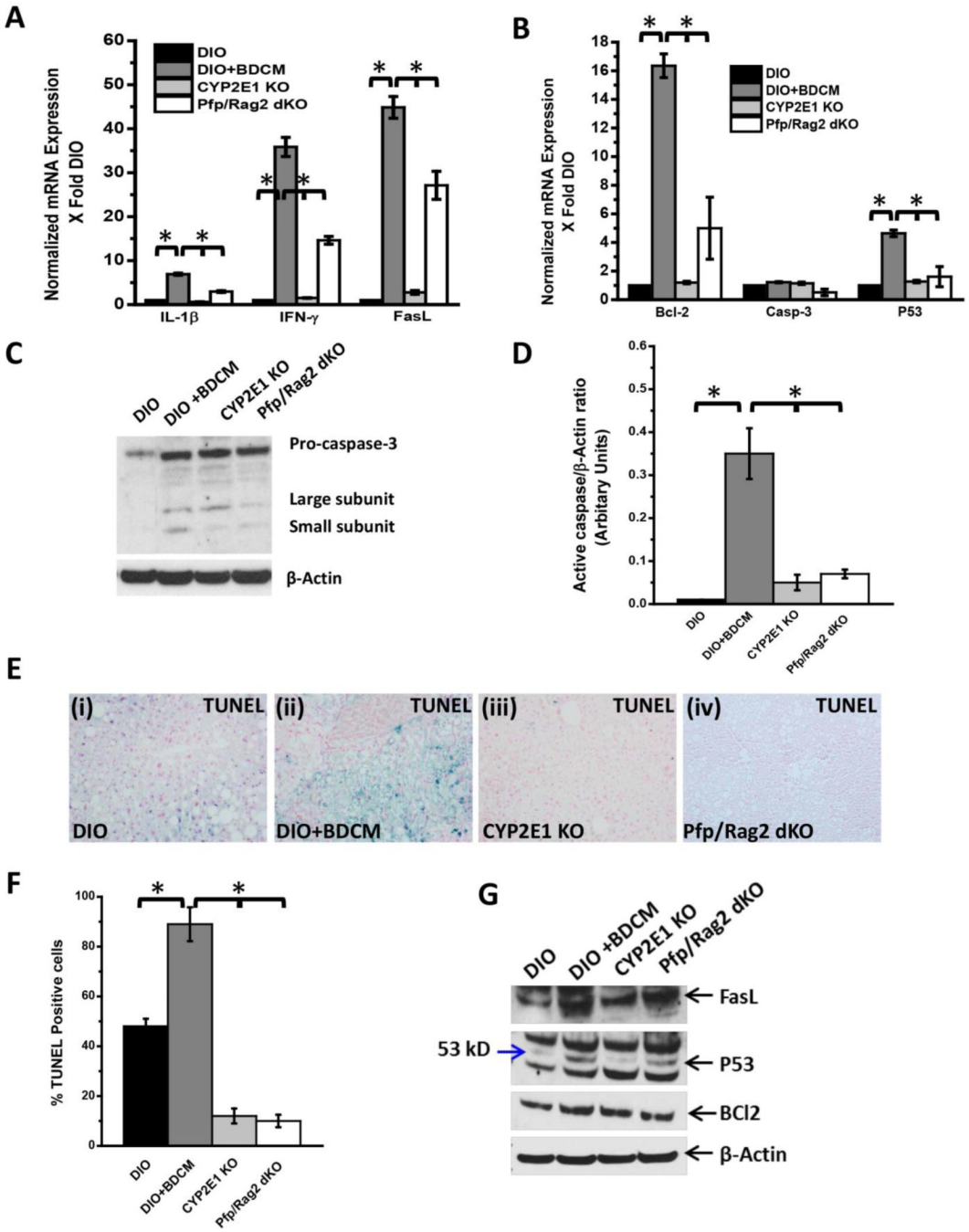

Fig.3.

A. mRNA expressions of IL-1β, IFN-γ and FasL from liver homogenates of dietinduced obese mouse (DIO), diet-induced obese mouse exposed to bromodichloromethane (DIO +BDCM), diet-induced obese mouse with CYP2E1 gene deletion and exposed to bromodichloromethane (CYP2E1 KO), and diet-induced obese mouse with Pfp/Rag2 dual gene deletion and exposed to bromodichloromethane (Pfp/Rag2 dKO). mRNA expressions had been assessed by quantitative real-time PCR (qRTPCR) and expressions in DIO +BDCM, CYP2E1 KO and Pfp/Rag2 dKO groups were normalized against mRNA expression in DIO group (* $P<0.05$). B. mRNA expressions of Bcl-2, Caspase-3 (Casp-3) and P53 from liver homogenates of DIO, DIO+BDCM, CYP2E1 KO and Pfp/Rag2 dKO

NIH-PA Author Manuscript

NIH-PA Author Manuscript

NIH-PA Author Manuscript

groups. mRNA expressions had been assessed by qRTPCR and expressions in DIO+BDCM, CYP2E1 KO and Pfp/Rag2 dKO groups were normalized against mRNA expression in DIO group (* $P<0.05$). C. Western Blot analysis of pro-caspase-3 and active-caspase-3 (large and small subunits) protein expression levels in liver homogenates from DIO, DIO+BDCM, CYP2E1 KO and Pfp/Rag2 dKO groups. The corresponding β-actin levels are shown in the lower panel. D. Band quantification analysis (arbitrary units) of active-caspase-3 (ratio to β-actin) from DIO, DIO+BDCM, CYP2E1 KO and Pfp/Rag2 dKO groups (bands shown in fig. 3C). E (i)–(iv). Number of apoptotic nuclei as shown by TUNEL staining in liver slices from DIO, DIO+BDCM, CYP2E1 KO and Pfp/Rag2 dKO groups respectively. Number of TUNEL positive cells identified by their blue-stained nuclei as against the nuclear fast red stained nuclei correspond to the number of apoptotic events. Images were taken in 20× magnification. F. Percentage of TUNEL positive cells (obtained by morphometry done on images from three separate microscopic fields) in DIO, DIO+BDCM, CYP2E1 KO and Pfp/Rag2 dKO groups (* $P<0.05$). Western blot analysis of apoptotic protein FasL, p53 and Bcl2 (From top down) from liver homogenates.

NIH-PA Author Manuscript
NIH-PA Author Manuscript
NIH-PA Author Manuscript

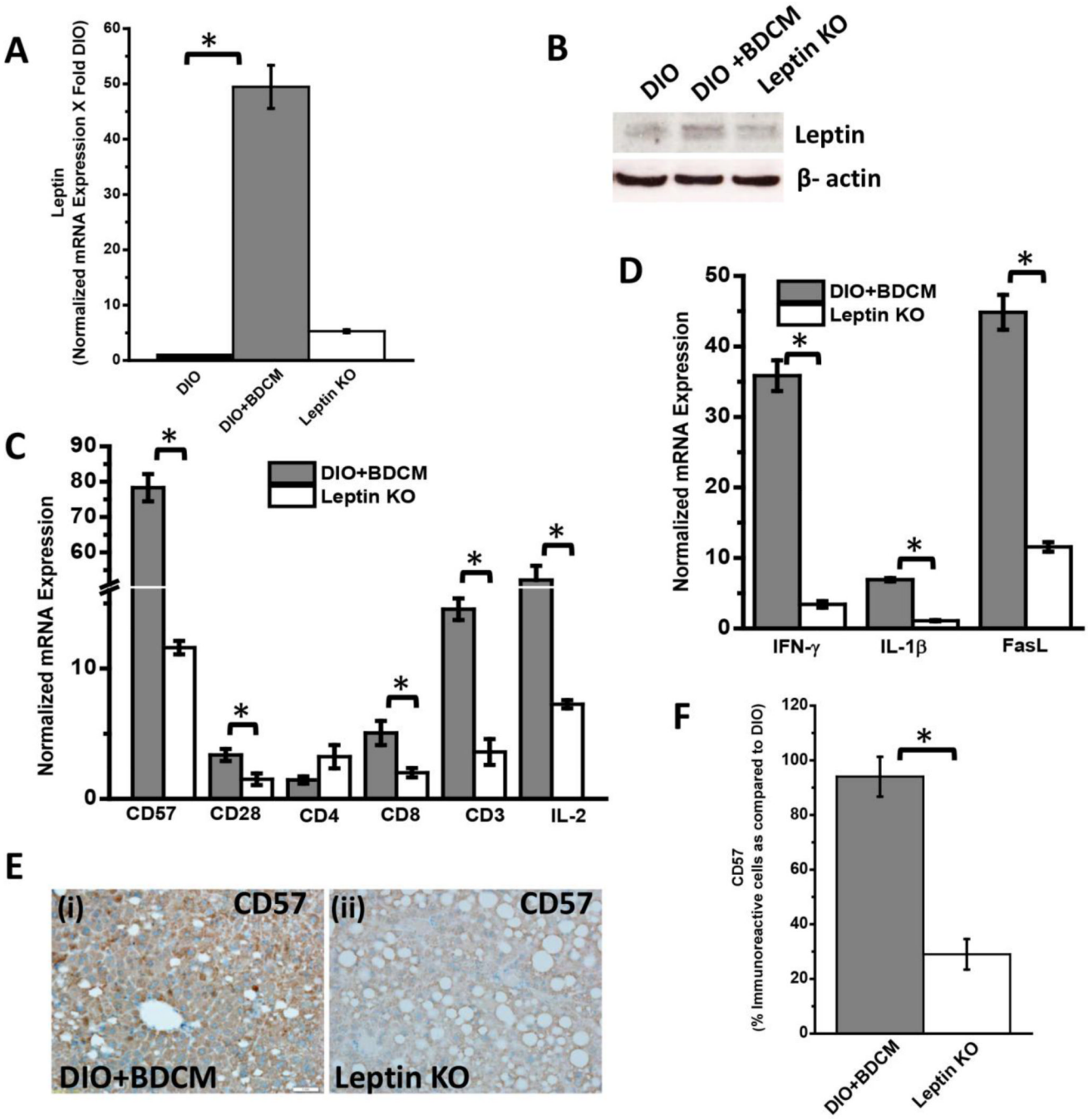

NIH-PA Author Manuscript
NIH-PA Author Manuscript
NIH-PA Author Manuscript

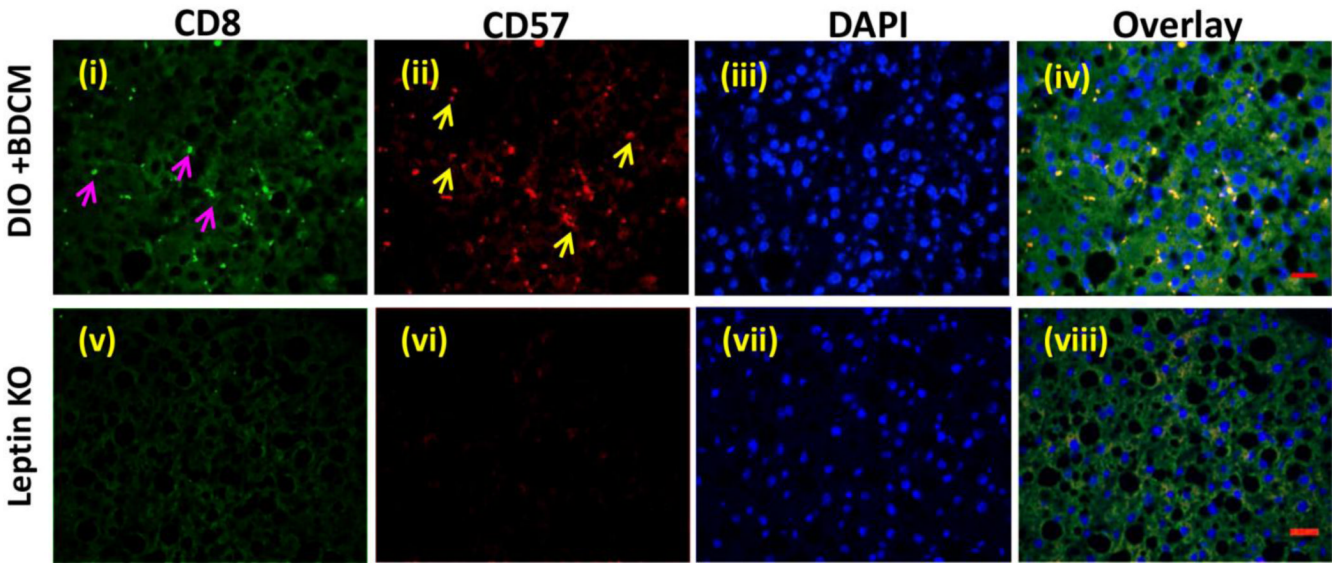

Fig.4.

A. mRNA expression of leptin from liver homogenates of diet-induced obese mouse (DIO), diet-induced obese mouse exposed to bromodichloromethane (DIO+BDCM) and diet-induced obese mouse with leptin gene deletion and exposed to bromodichloromethane (Leptin KO). mRNA expressions had been assessed by quantitative real-time PCR (qRTPCR) and expressions in DIO+BDCM and Leptin KO groups were normalized against mRNA expression in DIO group (* $P<0.05$). B. Western Blot analysis of leptin protein expression levels in liver homogenates from DIO, DIO+BDCM and Leptin KO groups. The corresponding β-actin levels are shown in the lower panel. C. mRNA expressions of CD57, CD28, CD4, CD8, CD3 and IL-2 from liver homogenates of DIO+BDCM and Leptin KO groups. mRNA expressions had been assessed by qRTPCR and expressions in DIO+BDCM and Leptin KO groups were normalized against mRNA expression in DIO group (* $P<0.05$). D. mRNA expressions of IFN-γ, IL-1β and FasL from liver homogenates of DIO+BDCM and Leptin KO groups. mRNA expressions had been assessed by qRTPCR and expressions in DIO+BDCM and Leptin KO groups were normalized against mRNA expression in DIO group (* $P<0.05$). E (i)–(ii). CD57 immunoreactivity as shown by immunohistochemistry in liver slices from DIO+BDCM and Leptin KO groups respectively. Images were taken in 20× magnification. F. Percentage of CD57 positive immunoreactive cells (obtained by morphometry done on images from three separate microscopic fields) in DIO+BDCM and Leptin KO groups compared to DIO group (* $P<0.05$). G. Immunofluorescence images for co-localization of CD57 (red) and CD8 (green) from liver sections of DIO+BDCM [(i)–(iv)] and Leptin KO[(v)–(viii)] groups. The images in the overlay panel on the extreme right depict co-localizations of CD57 and CD8 as revealed by the yellow regions. Images were taken in 40× magnification. The localizations of CD8 and CD57 are shown by pink and yellow arrows respectively.

NIH-PA Author Manuscript
NIH-PA Author Manuscript
NIH-PA Author Manuscript

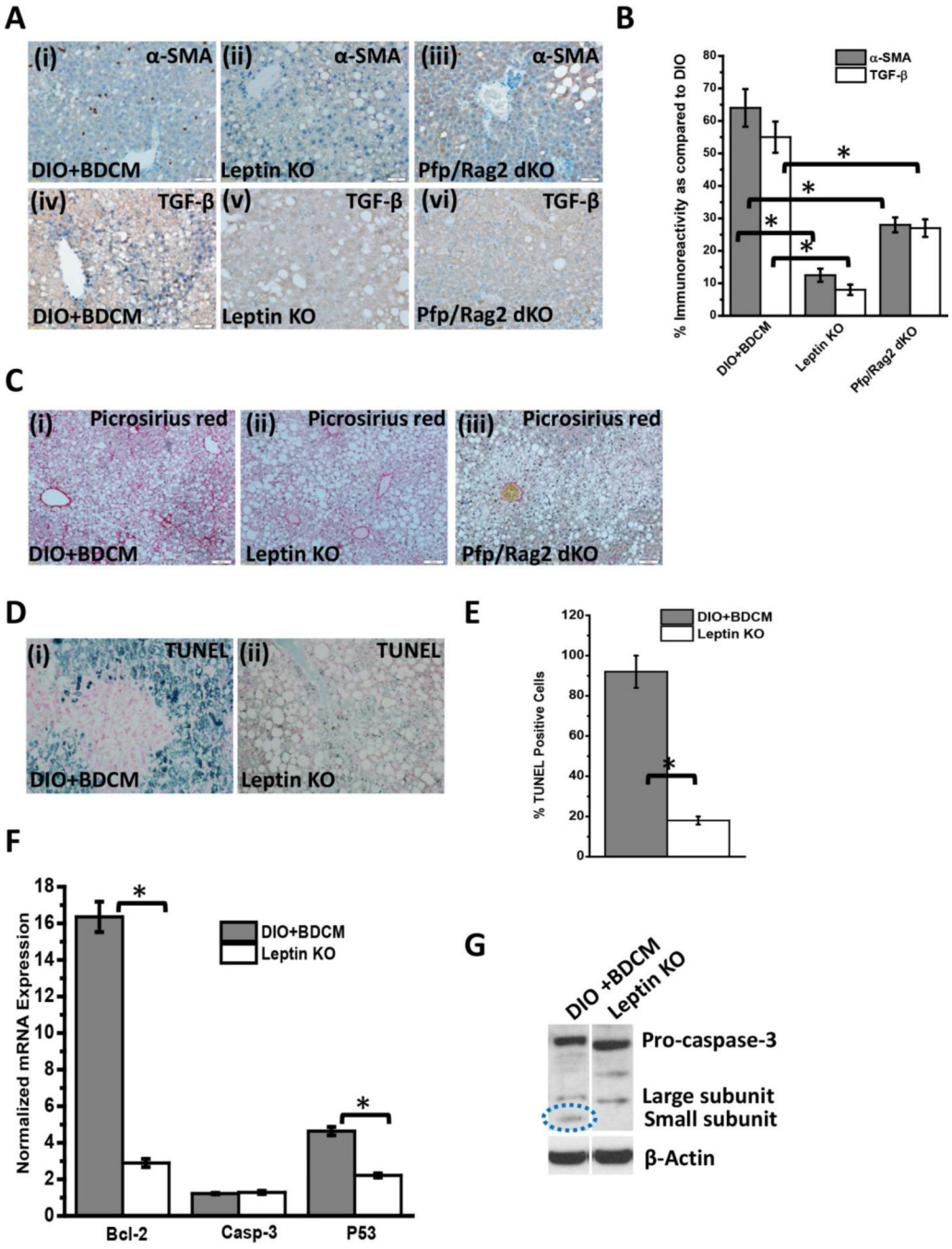

Fig.5.

A (i)–(iii). α-Smooth muscle actin (α-SMA) immunoreactivity as shown by immunohistochemistry in liver slices from diet-induced obese mouse exposed to bromodichloromethane (DIO+BDCM), diet-induced obese mouse with leptin gene deletion and exposed to bromodichloromethane (Leptin KO) and diet-induced obese mouse with Pfp/Rag2 dual gene deletion and exposed to bromodichloromethane (Pfp/Rag2 dKO) respectively. (iv)–(vi) TGF-β immunoreactivity as shown by immunohistochemistry in liver slices from DIO+BDCM, Leptin KO and Pfp/Rag2 dKO groups respectively. All images were taken in 20× magnification. B. Percentage of α-SMA positive and TGF-β positive immunoreactive cells (obtained by morphometry done on images from three separate

NIH-PA Author Manuscript

NIH-PA Author Manuscript

NIH-PA Author Manuscript

microscopic fields in each case) in DIO+BDCM, Leptin KO and Pfp/Rag2 dKO groups compared to DIO group (* $P<0.05$). C (i)–(iii). Macro- and micro-vescicular collagen deposition as shown by Picrosirius red staining in liver slices from DIO+BDCM, Leptin KO and Pfp/Rag2 dKO groups respectively. Images were taken in 10× magnification. D (i)–(ii). Number of apoptotic nuclei as shown by TUNEL staining in liver slices from DIO+BDCM and Leptin KO groups respectively. Number of TUNEL positive cells identified by their blue-stained nuclei as against the nuclear fast red stained nuclei correspond to the number of apoptotic events. Images were taken in 20× magnification. E. Percentage of TUNEL positive cells (obtained by morphometry done on images from three separate microscopic fields) in DIO+BDCM and Leptin KO groups (* $P<0.05$). F. mRNA expressions of Bcl-2, Caspase-3 (Casp-3) and P53 from liver homogenates of DIO+BDCM and Leptin KO groups. mRNA expressions had been assessed by quantitative real-time PCR (qRTPCR) and expressions in DIO+BDCM and Leptin KO groups were normalized against mRNA expression in DIO group (* $P<0.05$). G. Western Blot analysis of pro-caspase-3 and active-caspase-3 (large and small subunits) protein expression levels in liver homogenates from DIO+BDCM and Leptin KO groups. The corresponding β-actin levels are shown in the lower panel.

NIH-PA Author Manuscript

NIH-PA Author Manuscript

NIH-PA Author Manuscript

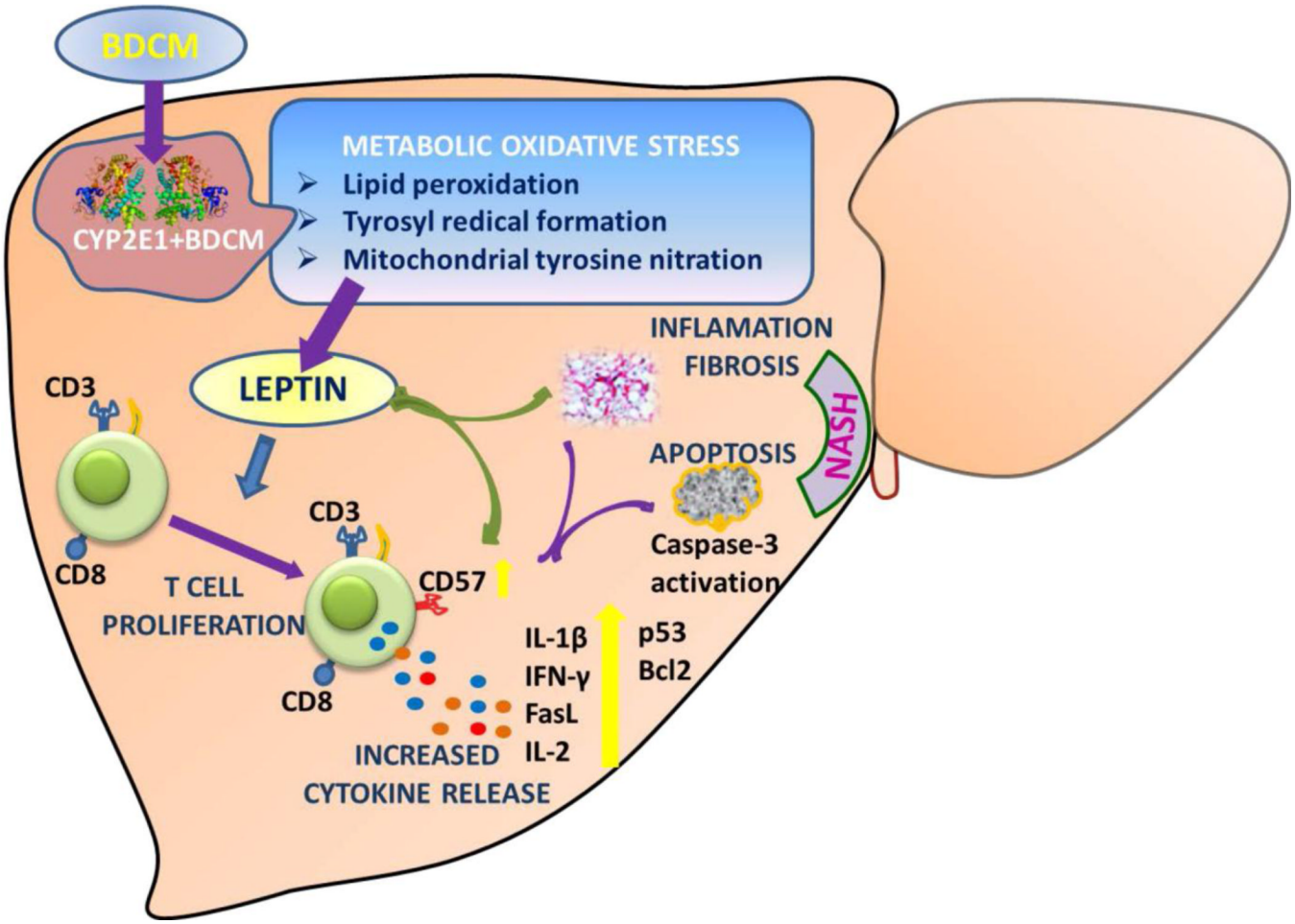

Fig.6.

Graphical representation of the role of CD8+veCD57+ve T cells in NASH pathogenesis. Metabolic oxidative stress mediated by the xenobiotic enzyme CYP2E1 increases hepatic leptin levels. Leptin causes an increased expression of CD57 on CD8+ve T cells and mediates release of proinflammatory cytokines with a concomitant increase of apoptosis in the liver. Inflammatory T cell signals causes increased fibrosis and contributes to NASH progression.